

# Organic matter determines the exchange of nutrients at sediment-water interface in coastal bays

Jiasen Zhong<sup>1</sup>, Ehui Tan<sup>1, 2\*</sup>, Chunwei Fu<sup>1</sup>, Guiyi Ma<sup>1</sup>, Yongkai Chang<sup>1</sup>, Zhixiong Huang<sup>1</sup>, Jingchao Yin<sup>1</sup>, Fengying Li<sup>1</sup>, Jianzhong Su<sup>1, 2</sup>, Min Xu<sup>1, 2</sup>, Zhenzhen Zheng<sup>1, 2</sup>, Jian'an Liu<sup>1, 2</sup>, Yu Han<sup>1, 2</sup>, Shuh-Ji Kao<sup>1, 2</sup>

<sup>1</sup> State Key Laboratory of Marine Resources Utilization in the South China Sea, School of Ecology and Environment and School of Marine Science and Engineering, Hainan University, Haikou 570228, China

<sup>2</sup> Collaborative Innovation Center of Marine Science and Technology, Hainan University, Haikou 570228, China

Received 3 January 2024; accepted 25 April 2024

© Chinese Society for Oceanography and Springer-Verlag GmbH Germany, part of Springer Nature 2025

## Abstract

The exchange of inorganic nutrients at the coastal sediment-water interface (SWI) plays a crucial role in regulating the nutrient budget in overlying water. The related studies mainly focus on the mid-to high-latitude regions, leaving a significant gap in the quantitative assessment of nutrient exchange and environmental controls at the SWI in low-latitude coastal regions. We quantitatively assess the exchange of inorganic nutrients at the SWI in three tropical bays (Dongzhai Harbor, Xiaohai Lagoon, Qinglan Harbor). Sediments act as a source of ammonium, phosphate, and silicate, but for nitrate, sediments can be both a source and sink, although with substantial spatial and temporal variations in their fluxes. Labile organic matter is a critical regulator for the fluxes of inorganic nutrients at the SWI. The sedimentary nutrients input with high N/P molar ratio will alter the nutrient stoichiometry to mitigate the nitrogen limitation in coastal waters. However, the internal sediment release in these tropical bays plays a relative weak role in contributing to the nutrient addition in comparison with the other external nutrient sources including riverine input, submarine groundwater discharge, and atmospheric deposition. According to the global compilation on SWI nutrient fluxes, we propose that water column primary production and external inputs to interpret the variation in exchange and fluxes of nutrients at the SWI in different ecosystems. Such a conceptual understanding of these chain biogeochemical processes involving external nutrient input, primary production, particulate organic matter settling, and the accumulation and release of inorganic nutrients in sediments will be helpful for the scientific-based pollution prevent and control in coastal waters.

**Key words** tropical bay, sediment-water interface, nutrient exchange, labile organic matter, source/sink

**Citation** Zhong Jiasen, Tan Ehui, Fu Chunwei, Ma Guiyi, Chang Yongkai, Huang Zhixiong, Yin Jingchao, Li Fengying, Su Jianzhong, Xu Min, Zheng Zhenzhen, Liu Jian'an, Han Yu, Kao Shuh-Ji. 2025. Organic matter determines the exchange of nutrients at sediment-water interface in coastal bays. *Acta Oceanologica Sinica*, 44(1): 72–85, doi: 10.1007/s13131-024-2416-6

## 1 Introduction

Dissolved inorganic nitrogen (DIN), inorganic phosphorus (DIP), and silicon (DSi), as the essential elements for the growth of phytoplankton and limiting factors for primary productivity, are important components of the

global marine biogeochemical cycles (Behrenfeld et al., 2006). With the development of industry and intensification of urbanization, the majority of fertilizers and wastewater discharge on land will ultimately deliver into coastal waters via riverine input, groundwater discharge, and atmospheric deposition, mitigating the nutrient limita-

Foundation item: The Major Science and Technology Plan of Hainan Province under contract No. ZDKJ2021008; the Hainan Provincial Natural Science Foundation of China under contract No. 623RC456; the Hainan Province Science and Technology Special Fund under contract Nos ZDYF2021SHFZ064 and ZDYF2022SHFZ056; the Collaborative Innovation Center of Marine Science and Technology in Hainan University under contract No. XTCX2022HYC19.

\*Corresponding author, E-mail: ehuitan@hainanu.edu.cn

<http://www.aosocean.com>  
E-mail: ocean2@hyxb.org.cn

tion to stimulate primary productivity and subsequently enhancing the coastal carbon sink (Mackenzie et al., 2002). In addition, aquaculture reclamation also contributes nutrients into coastal bays (Lin and Lin, 2022). However, these excess nutrients inevitably lead to environmental issues such as eutrophication and the related algal blooms, hypoxia, and acidification in coastal waters (Devlin and Brodie, 2023). Therefore, understanding the sources of major nutrients and their fates in nearshore environments will contribute to the water pollution prevention at regional and global scales.

Coastal sediments are important sites for carbon sink. Both terrigenous and marine produced organic matter buries in coastal sediments and its degradation drives a series of carbon and nitrogen biogeochemical cycles, which play significant roles in regulating the spatiotemporal distributions and budgets of nutrients in overlying water via the sediment-water interface (SWI), particularly in nearshore environments with a shallow water depth (Burdige, 2011). For instance, ammonium ( $\text{NH}_4^+\text{-N}$ ) produced from sedimentary organic matter respiration accumulates in porewater and diffuse upward across the SWI to the overlying water, which can promote primary production and may potentially cause endogenous pollution. Conversely, the microbial-mediated processes including denitrification and anaerobic ammonia oxidation at the SWI eliminate  $\text{NO}_x^-\text{-N}$  (nitrite plus nitrate) to reduce their accumulation in coastal waters, acting as a buffer against eutrophication (Denis and Grenz, 2003; Qiu et al., 2016; Zhang et al., 2014, 2023). Thus, the source and sink processes of major nutrients (DIN, DIP and DSi) and their fluxes at the SWI play a crucial role in balancing nutrient budgets and maintenance of primary productivity.

The SWI is one of the key interfaces in aquatic ecosystems, more and more studies have focused on the investigation of nutrient exchange fluxes and their environmental factors at the SWI in various coastal habitats, including estuaries, bays, lagoons and continental shelves (Ben Mna et al., 2022; Lehrter et al., 2012; Mu et al., 2017). Recent researches have indicated that abiotic and biotic environmental factors in overlying water (temperature, dissolved oxygen, and nutrient concentrations) and sediments (porosity, organic carbon-nitrogen contents, C/N molar ratio, and microbial communities) affect the nutrient exchange at the SWI by influencing both physical and biochemical processes such as adsorption-desorption, dissolution, diffusion, remineralization, and microbial activities (Boynton et al., 2018; Dadi et al., 2023; Wang et al., 2023; Zhao et al., 2018; Zhou et al., 2022; Zhu et al., 2023). However, most of these studies have been concentrated in mid-to high-latitude regions, leaving a significant gap in the quantitative assessment of nutrient exchange and environmental controls at the SWI in low-latitude regions (Boynton et al., 2018). The low-latitude ecosystems are experience greater and more sensitive to climate change (Pinsky et al., 2019). Higher temperatures

will favor primary production and enhance sediment carbon-nitrogen biogeochemical processes, potentially altering the source-sink of nutrients, and amplifying or inhibiting their fluxes at the SWI. In addition, the relative importance between internal exchange at the SWI and external inputs (such as riverine delivery, atmospheric deposition, and groundwater discharge) in coastal regions, especially in shallow water ecosystems remains underexplored (Fennel and Testa, 2019).

Hainan Island is located in the southern China and experiences a typical tropical monsoon climate, hosting diverse nearshore ecosystem types. We conducted field investigations in different seasons in Dongzhai Harbor, Xiaohai Lagoon, and Qinglan Harbor, representing the mangrove, lagoon, and bay-type nearshore shallow-water ecosystems in low latitude regions, respectively (Fig. 1). Bottom water, surface sediments (1 cm), and pore water were collected (1) to quantify the exchange and fluxes of inorganic nutrients (DIN, DIP, and DSi) at the SWI, (2) to identify the key environmental factors. Finally, historical data on regional external inputs were integrated to comprehensively assess the relative importance of internal sediment release in the nutrient budget in these coastal shallow water ecosystems.

## 2 Sampling and methods

### 2.1 Study area

Dongzhai Harbor (DZG, Figs 1b and c) is the first mangrove reserve in China with a depth ranging from approximately 4 m to 12 m. The annual average precipitation is 1 700 mm, and the mean annual temperature is 23.8°C. DZG experiences an irregular semidiurnal tide with a tidal height of 1.5–2.0 m (Li et al., 2017). Xiaohai (XH, Fig. 1d) is the largest lagoon in Hainan Province with an area of approximately 44 km<sup>2</sup> and a water depth of 1.5–4 m (Gong et al., 2008). Increasing human activities exert a seasonal eutrophication in the southern and central parts of XH, while the water quality has gradually improved after banning aquaculture in recent years (Gong et al., 2008; Luo et al., 2022). Qinglan Harbor (QLG, Fig. 1e) exhibits a funnel-shaped entrance with a narrow mouth and wide interior. The average water depth is approximately 1 m within the bay and 2–3 m in the southwest near the entrance. QLG has an annual average temperature of 23.9°C and an annual average rainfall of 1 799.4 mm (Chen et al., 2022). This region is subject to intensive port trade and aquaculture activities throughout the year, exerting a severe impact on the local ecosystems (Chen and Teng, 1996; Zhen et al., 2019).

### 2.2 Sample collection and pretreatment

Sampling cruises at DZG were conducted in January and May 2022, representing winter and summer, respectively (Figs 1b and c). The sampling campaigns were only carried out in summer (June 2022) in the XH and QLG

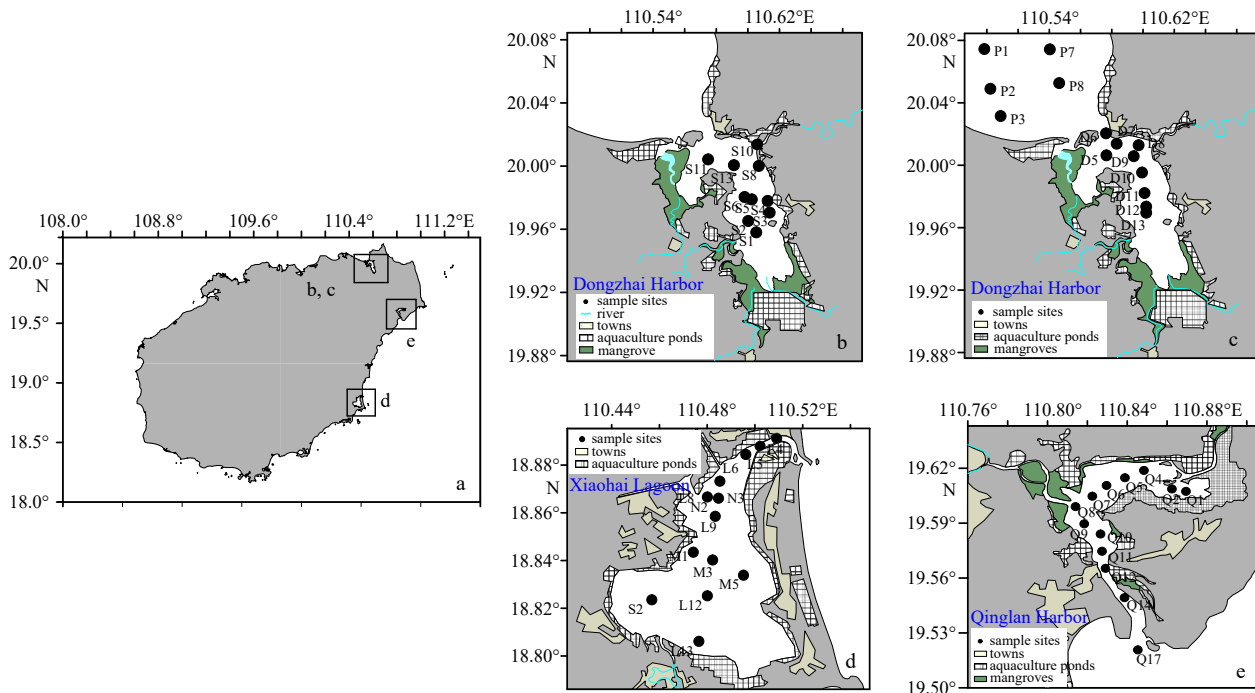


**Fig. 1.** Map of sampling stations at Dongzhai Harbor in winter and summer, Xiaohai Lagoon and Qinglan Harbor in summer.

(Figs 1d and e). All samplings were completed during the low tide and there was no rainfall before our campaigns. The fundamental environmental parameters including water depth, temperature, salinity and dissolved oxygen (DO) at each station were measured on-site using a Conductivity-Temperature-Depth profiler. Bottom water was collected at 1 m above the sediment by using a portable water sampler. The water samples were filtered through 0.45  $\mu\text{m}$  acetate fiber membranes and preserved in 50 mL centrifuge tubes at  $-20^{\circ}\text{C}$  for the determination of inorganic nutrient concentrations, including  $\text{NH}_4^+\text{-N}$ ,  $\text{NO}_x^-\text{-N}$ , DIP, and DSi. Sediment samples were collected using a grab-type sampler and the surface sediments (1 cm) were then transferred into a glovebox with an anaerobic environment to avoid the oxidation of  $\text{NH}_4^+\text{-N}$ . One part of these sediments was directly collected into 50 mL centrifuge tubes and then centrifuged, then the supernatant porewater was filtered and preserved at  $-20^{\circ}\text{C}$  for nutrient analysis. The remaining surface sediments were collected for the determination of porosity, Total organic carbon content (TOC), Total nitrogen content (TN), carbon-nitrogen ratio (C/N), and chlorophyll concentration.

### 2.3 Chemical analysis

The concentrations of  $\text{NO}_x^-\text{-N}$ ,  $\text{NH}_4^+\text{-N}$ , DIP, and DSi in bottom water and pore water were determined using a AA3 continuous flow analyzer with detection limits of 0.01  $\mu\text{mol/L}$ , 0.06  $\mu\text{mol/L}$ , 0.09  $\mu\text{mol/L}$ , 0.03  $\mu\text{mol/L}$ , and 0.15  $\mu\text{mol/L}$ , respectively (Liu et al., 2009). A known weight and volume of wet sediment was freeze-dried to determine the porosity (Boudreau, 1997). Then the dry sediment sample was treated with 1  $\mu\text{mol/L}$  HCl to re-

move inorganic carbon. After washing the sample with deionized water to neutrality, the sample was dried again and applied for TOC and TN measurement by using an Elemental Analyzer (EA) (Tan et al., 2019). The C/N molar ratio was then calculated according to the TOC and TN contents. The chlorophyll *a* (Chl *a*) concentration in sediment was extracted by acetone and then analyzed using spectrophotometry (Pinckney et al., 1994).

### 2.4 Determination of nutrient diffusion fluxes at sediment-water interface

The diffusive fluxes of  $\text{NO}_x^-\text{-N}$ ,  $\text{NH}_4^+\text{-N}$ , DIP, and DSi at the SWI were calculated according to the Fick's first law (Boudreau, 1997).

$$F = \varphi \cdot D \frac{\partial c}{\partial z}, \quad (1)$$

where  $F$  represents the nutrient diffusion flux;  $\varphi$  denotes the surface sediment porosity;  $\frac{\partial c}{\partial z}$  represents the concentration gradient at the sediment-water interface, the interface depth was set to 1 cm. The diffusion coefficient ( $D$ ) in the sediment can be calculated using the following equations (Ullman and Aller, 1982):

$$D = \varphi D_0, \quad \varphi < 0.7, \quad (2)$$

$$D = \varphi^2 D_0, \quad \varphi > 0.7. \quad (3)$$

where  $D_0$  represents the ideal diffusion coefficient of the substance in an infinitely dilute solution. In this study, the

ideal diffusion coefficients of  $\text{NO}_x^-$ -N,  $\text{NH}_4^+$ -N, DIP and  $\text{DSi}$  were set to  $1.91 \times 10^{-7}$  cm/s,  $1.98 \times 10^{-7}$  cm/s,  $7.34 \times 10^{-6}$  cm/s,  $1.00 \times 10^{-7}$  cm/s, respectively (Nriagu, 1979). Note that the positive values of the flux indicate that the sediments release nutrients into the overlying water, while the negative values represent the sediments act as a sink for nutrients diffusing from the overlying water to the sediments.

## 2.5 Statistic analysis

A one-way analysis of variance (ANOVA) was performed to examine the spatial difference in environmental parameters and nutrient diffusive fluxes. Pearson correlation was applied to test the SWI fluxes and different environmental factors. All statistical analyses were conducted at a 0.05 significance level using Statistical Package of Social Sciences (SPSS, version-19.0).

## 3 Results

### 3.1 Basic environmental parameters

During the sampling period, the water depth in winter

DZG, summer DZG, XH and QLG ranged from 1.0–4.0 m, 0.9–11.0 m, 0.5–4.2 m, and 1.3–7.3 m, respectively (Fig. 2a). The bottom water temperature in DZG during winter [20.6–21.3°C, averaging  $(20.8 \pm 0.2)^\circ\text{C}$ ] was significantly lower than the summer temperatures [25.6–28.8°C, averaging  $(26.8 \pm 1.0)^\circ\text{C}$ ]. The average bottom water temperatures in XH [ $(30.1 \pm 2.7)^\circ\text{C}$ ] and QLG [ $(29.5 \pm 1.35)^\circ\text{C}$ ] were comparable, but both were slightly higher than that in DZG during the same season (Fig. 2b). The bottom water salinity in DZG showed a small variation between winter and summer with a range of 27.9–32.0 (average  $30.8 \pm 1.4$ ) and 25.7–32.3 (average  $30.6 \pm 2.3$ ), respectively (Fig. 2c). In contrast, the salinity in XH and QLG exhibited a broader range, spanning from 10.7 to 33.0 and 15.9 to 33.1, respectively (Fig. 2c). The bottom water DO concentrations in DZG during winter ( $283.1 \pm 3.9$   $\mu\text{mol/L}$ ) were significantly higher than those during the other three cruises, including DZG [ $(213.4 \pm 5.2)$   $\mu\text{mol/L}$ ], XH [ $(252.2 \pm 46.9)$   $\mu\text{mol/L}$ ] and QLG [ $(185.7 \pm 12.4)$   $\mu\text{mol/L}$ ] in summer (Fig. 2d).

For surface sediment properties, the porosity in winter DZG, summer DZG, XH and QLG varied from 0.47 to 0.86, 0.38 to 0.65, 0.39 to 0.81, and 0.46 to 0.84, respec-

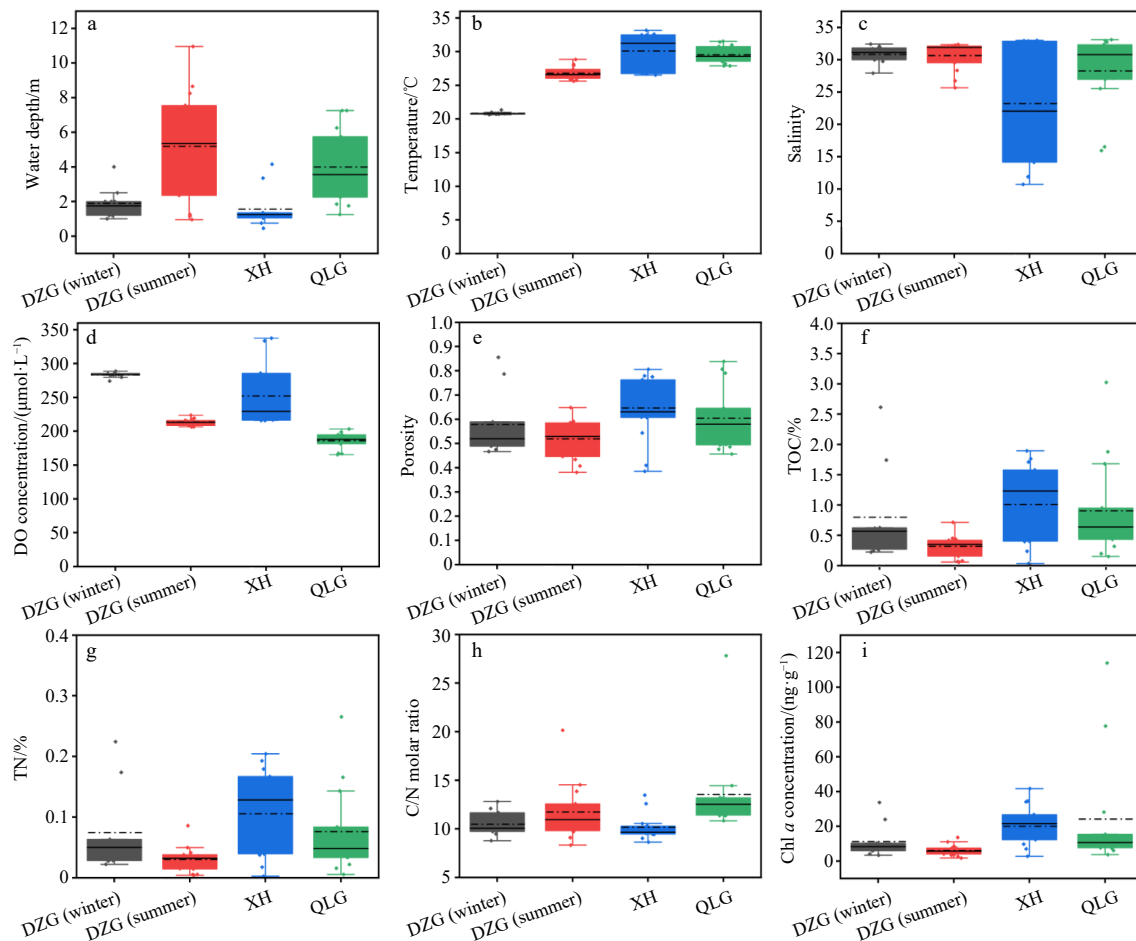


**Fig. 2.** The spatial distribution of environmental parameters in the overlying water and sediments during the four cruises. Subfigures (a–i) denote the water depth, temperature, salinity, DO, porosity, TOC, TN, C/N molar ratio and Chl *a* concentration, respectively. The solid and dashed lines represent the median and average of values, respectively.

tively (Fig. 2e). The TOC and TN contents showed a similar spatial variation during the four sampling campaigns (Figs 2f and g). The highest and lowest organic matter contents were observed in XH and DZG during summer, with average values of  $1.01\% \pm 0.65\%$  and  $0.31\% \pm 0.19\%$  for TOC,  $0.11\% \pm 0.07\%$  and  $0.03\% \pm 0.02\%$  for TN, respectively. Both the TOC and TN contents were comparable in winter DZG ( $0.80\% \pm 0.77\%$  for TOC and  $0.07\% \pm 0.07\%$  for TN) and in summer QLG ( $0.91\% \pm 0.82\%$  for TOC and  $0.08\% \pm 0.07\%$  for TN). The highest C/N ratio occurred in QLG with a range of 10.8 to 27.8 (average  $13.5 \pm 4.4$ ), followed by the summer DZG (8.3–20.1, average  $11.8 \pm 3.1$ ), winter DZG (8.8–12.8, average  $10.5 \pm 1.3$ ), and summer XH (8.6–13.5, average  $10.2 \pm 1.4$ ; Fig. 2h). The average sediment Chl *a* concentrations in XH and QLG during summer were ( $20.0 \pm 11.8$ ) ng/g and ( $24.2 \pm 33.2$ ) ng/g, respectively, which were 2–4 folds of those in winter DZG [( $11.3 \pm 9.8$ ) ng/g] and summer DZG [( $5.7 \pm 3.1$ ) ng/g] (Fig. 2i). Regardless

of the sampling cruises, the sediment TOC and TN content, C/N molar ratios, and Chl *a* content exhibited significant spatial variations among the four cruises (*p* values of 0.015, 0.013, 0.002, and 0.001, respectively).

### 3.2 Spatiotemporal distribution of nutrient concentration in bottom water

The highest  $\text{NO}_x^-$ -N concentrations during the four cruises were observed in DZG during winter with a range of 7.4–26.7  $\mu\text{mol/L}$  [average ( $13.1 \pm 6.0$ )  $\mu\text{mol/L}$ ; Fig. 3a], followed by the summer DZG ranging from 2.8  $\mu\text{mol/L}$  to 14.9  $\mu\text{mol/L}$  [average ( $7.5 \pm 3.9$ )  $\mu\text{mol/L}$ ; Fig. 3c]. Relatively, the  $\text{NO}_x^-$ -N concentrations in the XH and QLG were one order of magnitude lower with a range of 0.1–4.2  $\mu\text{mol/L}$  and 0.1–0.6  $\mu\text{mol/L}$ , respectively (Figs 3e, i). For the bottom water  $\text{NH}_4^+$ -N, comparable concentrations were observed in DZG during winter and summer with a range of 1.8–13.6  $\mu\text{mol/L}$  and 0.5–9.9  $\mu\text{mol/L}$ , respectively (Figs 3b, d), followed by the summer QLG with concentration of 0.3–5.6  $\mu\text{mol/L}$

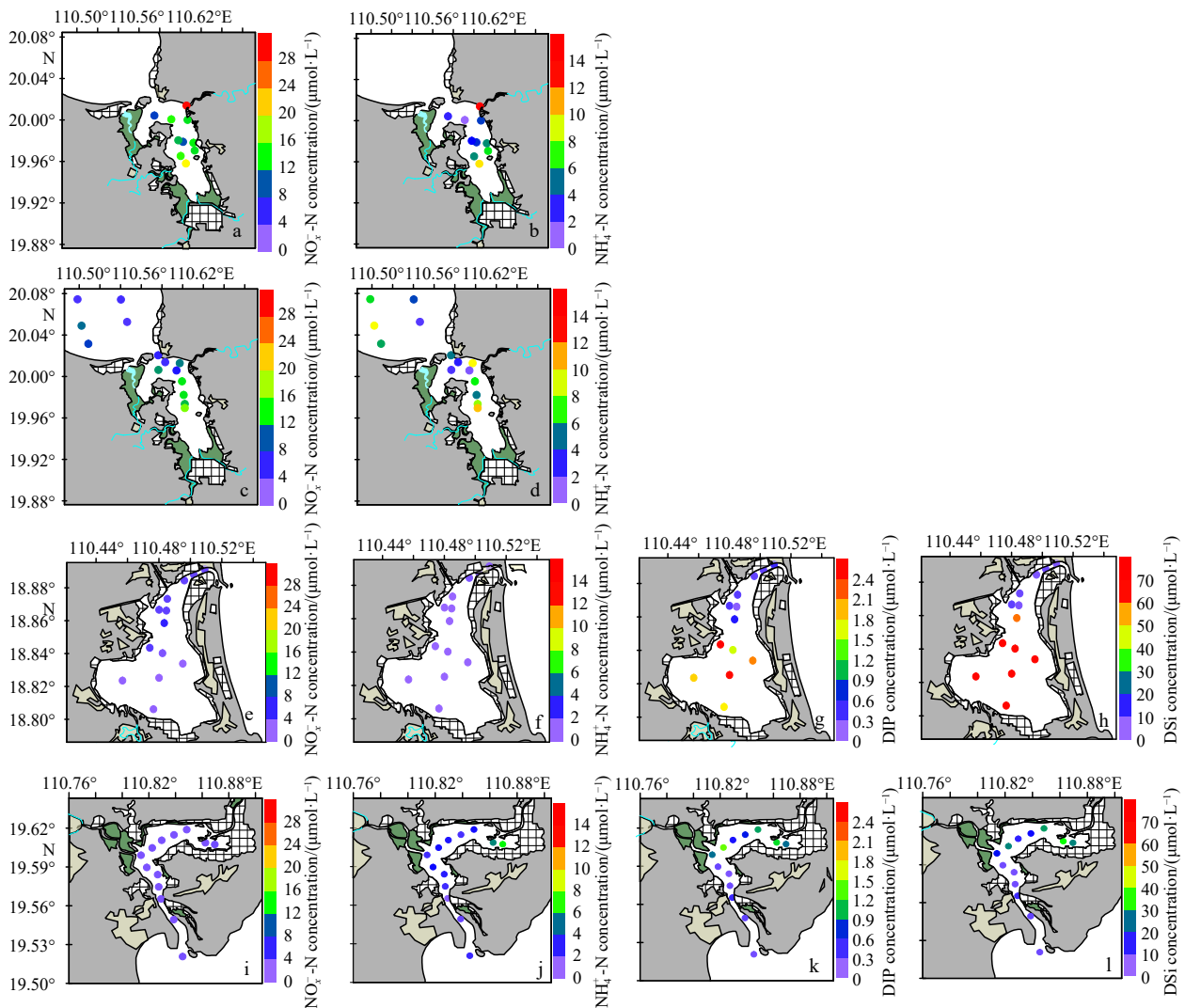


**Fig. 3.** Spatiotemporal distribution of nutrient concentration in bottom water. Subfigures a–b, c–d, e–h, and i–l represent the cruises in winter DZG, summer DZG, XH, and QLG, respectively. Subfigures from the first to fourth column represent the  $\text{NO}_x^-$ -N,  $\text{NH}_4^+$ -N, DIP, DSi concentrations, respectively, unit in  $\mu\text{mol/L}$ .

(Fig. 3j). The lowest  $\text{NH}_4^+\text{-N}$  concentrations occurred during the cruise in XH with concentration of 0.2–0.5  $\mu\text{mol/L}$  (Fig. 3f). Overall, the  $\text{NO}_x^-\text{-N}$  predominated the forms of DIN in winter DZG, summer DZG, and the XH, while in QLG,  $\text{NH}_4^+\text{-N}$  was the primary species for DIN.

The bottom water DIP and DSi concentrations in DZG during winter and summer were not measured due to some objective reasons. The DIP concentrations in XH (with a range of 0.05–2.5  $\mu\text{mol/L}$ , average  $(1.0 \pm 0.9)$   $\mu\text{mol/L}$ ; Fig. 3g) were nearly two-fold of those in QLG (0.1–1.3  $\mu\text{mol/L}$ , average  $(0.5 \pm 0.4)$   $\mu\text{mol/L}$ ; Fig. 3k). The concentrations of DSi in XH and QLG varied from 2.5  $\mu\text{mol/L}$  to 65.5  $\mu\text{mol/L}$  [average  $(35.8 \pm 31.2)$   $\mu\text{mol/L}$ ] and from 3.2  $\mu\text{mol/L}$  to 28.4  $\mu\text{mol/L}$  [average  $(12.2 \pm 8.7)$   $\mu\text{mol/L}$ ], respectively (Figs 3h, l).

### 3.3 Spatiotemporal distribution of nutrient concentration in porewater

The concentrations of  $\text{NO}_x^-\text{-N}$  in the surface porewa-

ter varied from 0.7  $\mu\text{mol/L}$  to 4.5  $\mu\text{mol/L}$ , 1.7  $\mu\text{mol/L}$  to 73.5  $\mu\text{mol/L}$ , 0.1  $\mu\text{mol/L}$  to 19.9  $\mu\text{mol/L}$ , and 0.5  $\mu\text{mol/L}$  to 46.5  $\mu\text{mol/L}$  in winter DZG, summer DZG, XH, and QLG, respectively (Figs 4a, e, i and m). Excepting for some extremely high values, the average  $\text{NO}_x^-\text{-N}$  concentrations were relatively consistent across the four cruises with values of  $(2.1 \pm 1.5)$   $\mu\text{mol/L}$ ,  $(3.5 \pm 1.9)$   $\mu\text{mol/L}$ ,  $(1.2 \pm 1.1)$   $\mu\text{mol/L}$ , and  $(1.2 \pm 1.9)$   $\mu\text{mol/L}$ , respectively. The concentrations of  $\text{NH}_4^+\text{-N}$  in porewater were 2–3 orders of magnitude higher than  $\text{NO}_x^-\text{-N}$  concentrations with concentrations of 11.1–75.4  $\mu\text{mol/L}$ , 14.3–253.5  $\mu\text{mol/L}$ , 48.9–698.1  $\mu\text{mol/L}$ , and 34.3–875.4  $\mu\text{mol/L}$  in winter DZG, summer DZG, XH, and QLG, respectively (Figs 4b, f, j and n). Obviously,  $\text{NH}_4^+\text{-N}$  was the dominant DIN species in sediment porewater throughout the four cruises.

The DIP concentrations in porewater were nearly in the same magnitude with concentrations of 1.4–3.3  $\mu\text{mol/L}$ , 2.3–8.5  $\mu\text{mol/L}$ , 1.2–29.0  $\mu\text{mol/L}$ , and 0.7–20.4  $\mu\text{mol/L}$  in winter DZG, summer DZG, XH, and

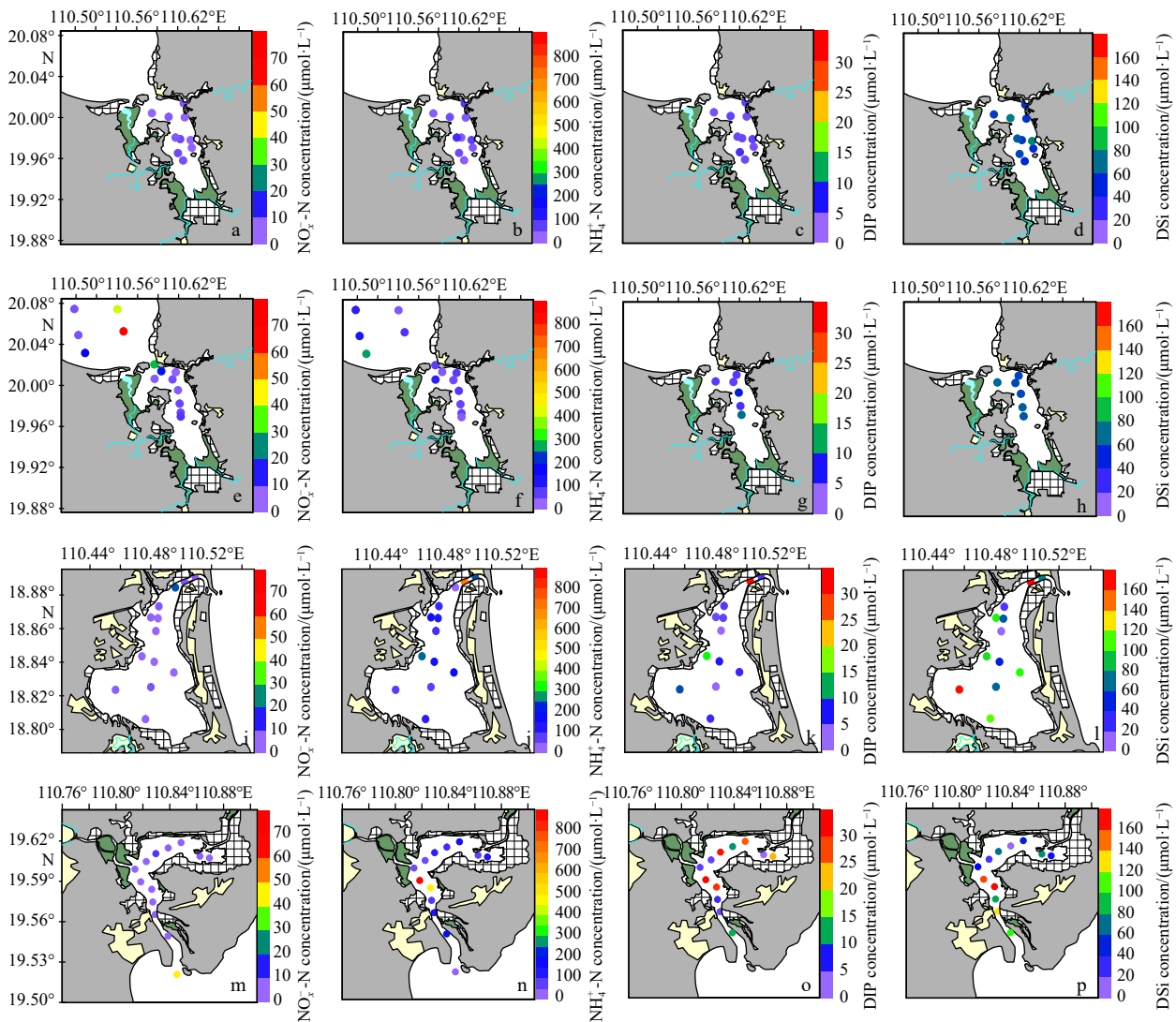


**Fig. 4.** Spatiotemporal distribution of nutrient concentration in porewater. Subfigures a–d, e–h, i–l, and m–p represent the cruises in winter DZG, summer DZG, XH, and QLG, respectively. Subfigures from the first to fourth column represent the  $\text{NO}_x^-\text{-N}$ ,  $\text{NH}_4^+\text{-N}$ , DIP and DSi concentrations, respectively.

QLG, respectively (Figs 4c, g, k and o). On average, the highest and lowest porewater DIP concentrations occurred during the cruises in summer QLG [(9.3 ± 7.7) μmol/L; Fig. 4o)] and winter DZG [(2.0 ± 0.6) μmol/L; Fig. 4c), respectively. For the DSi concentrations, the highest concentration appeared in summer XH [44.1–163.1 μmol/L, average (98.8 ± 35.9) μmol/L], followed by summer QLG [36.2–159.4 μmol/L, average (88.0 ± 38.5) μmol/L], summer DZG [48.9–57.9 μmol/L, average (52.6 ± 3.7) μmol/L], and winter DZG [41.5–66.3 μmol/L, average (49.9 ± 8.9) μmol/L] (Figs 4d, h, l and p).

## 4 Discussion

### 4.1 The fluxes of nutrient exchange at SWI

We observed distinct source/sink features for  $\text{NO}_x^-$ -N at the SWI in these three tropical bays. In DZG, the SWI consistently acts as a sink for  $\text{NO}_x^-$ -N throughout the sampling sites with fluxes of  $-111.2 \mu\text{mol}/(\text{m}^2\cdot\text{d})$

to  $-12.0 \mu\text{mol}/(\text{m}^2\cdot\text{d})$  and an average of  $(-61.2 \pm 34.0) \mu\text{mol}/(\text{m}^2\cdot\text{d})$  during the cruise in winter (Fig. 5a). During the summer cruise in DZG, negative fluxes for  $\text{NO}_x^-$ -N [ $-54.0 \mu\text{mol}/(\text{m}^2\cdot\text{d})$  to  $-4.3 \mu\text{mol}/(\text{m}^2\cdot\text{d})$ ] were obtained at the SWI within the bay, suggesting that the bay sediments act as a sink for  $\text{NO}_x^-$ -N. However, the sediments release  $\text{NO}_x^-$ -N to the overlying water with fluxes ranging from  $0.9 \mu\text{mol}/(\text{m}^2\cdot\text{d})$  to  $199.6 \mu\text{mol}/(\text{m}^2\cdot\text{d})$  outside the bay (Fig. 5c). The  $\text{NO}_x^-$ -N fluxes at the SWI in XH varied from  $-24.6 \mu\text{mol}/(\text{m}^2\cdot\text{d})$  to  $49.1 \mu\text{mol}/(\text{m}^2\cdot\text{d})$  with negative values observed in the central of lagoon (Fig. 5e). In the QLG, the sediments mainly serve as a source for  $\text{NO}_x^-$ -N, with fluxes ranging from  $-0.11 \mu\text{mol}/(\text{m}^2\cdot\text{d})$  to  $186.0 \mu\text{mol}/(\text{m}^2\cdot\text{d})$  (Fig. 5i). Coastal sediments function as hotspots for nitrogen removal with a proportion of 50%–70% to total nitrogen loss in marine environments (Seitzinger et al., 2006). The substrates for sediment nitrogen removal were primarily derived from the nitrification-produced nitrate in aerobic sediments and the physical-diffused nitrate from overlying water (Thamdrup and Dalsgaard, 2008), with the latter is a more im-

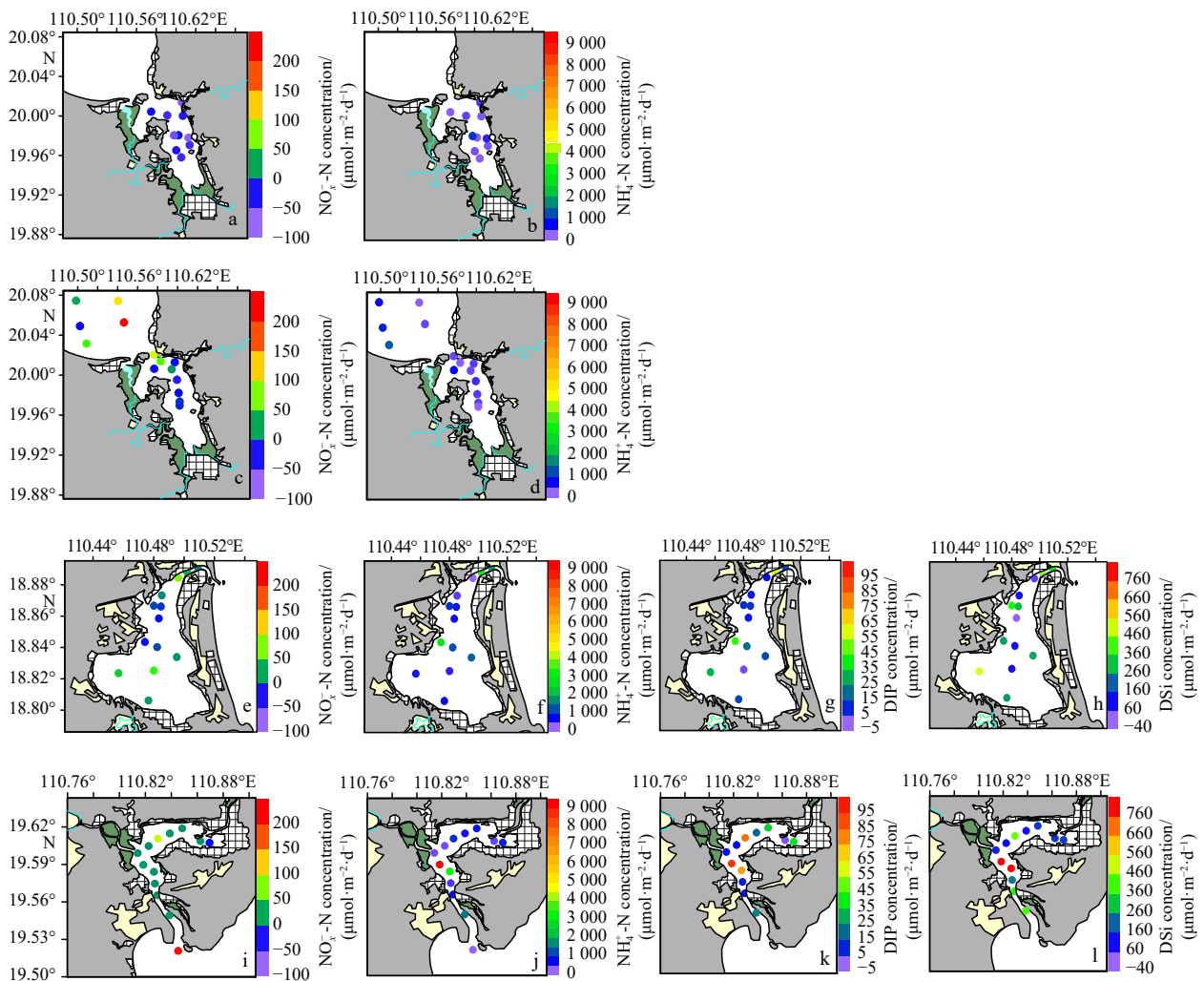


**Fig. 5.** Spatial distribution of nutrient diffusion fluxes in sediment-water interface, unit:  $\mu\text{mol}/(\text{m}^2\cdot\text{d})$  (a–b and c–d represent the cruises of Dongzhai Harbor in winter and summer, respectively, e–h represent the cruise of Xiaohai Lagoon, i–l represent the cruise of Qinglan Harbor in summer).

portant pathway particularly in nitrate abundant environments (Devol, 2015). In this study, the sediment within the DZG consistently acts as a sink for  $\text{NO}_x^-$ -N regardless of the season, directly indicating the key role of sediment in removing nitrate from the overlying water in eutrophic environments. However, the finding of nitrate release at the SWI in XH and QLG implies that a strong nitrification occurs in surface sediments. This sediment nitrification-produced nitrate may diffuse downward to support nitrogen removal in anaerobic layer and upward to the overlying water to fuel primary production.

The SWI was consistently a source for  $\text{NH}_4^+$ -N, DIP and DSi regardless of seasons and regions, even though their fluxes showed significant spatial variations ( $p < 0.05$ ). The  $\text{NH}_4^+$ -N fluxes in winter DZG, summer DZG, XH, and QLG varied in range of 51.6–807.7  $\mu\text{mol}/(\text{m}^2 \cdot \text{d})$ , 18.9–1 159.9  $\mu\text{mol}/(\text{m}^2 \cdot \text{d})$ , 204–3 520.9  $\mu\text{mol}/(\text{m}^2 \cdot \text{d})$ , and 12.4–8 790.6  $\mu\text{mol}/(\text{m}^2 \cdot \text{d})$ , with average values of  $(207.3 \pm 248.2) \mu\text{mol}/(\text{m}^2 \cdot \text{d})$ ,  $(317.9 \pm 311.0) \mu\text{mol}/(\text{m}^2 \cdot \text{d})$ ,  $(1 067.9 \pm 945.6) \mu\text{mol}/(\text{m}^2 \cdot \text{d})$ , and  $(1 378.6 \pm 2 444.4) \mu\text{mol}/(\text{m}^2 \cdot \text{d})$ , respectively (Figs 5b, d, f and j). The average fluxes of both DIP and DSi in QLG [ $(28.8 \pm 32.8) \mu\text{mol}/(\text{m}^2 \cdot \text{d})$  for DIP and  $(294.2 \pm 283.2) \mu\text{mol}/(\text{m}^2 \cdot \text{d})$  for DSi] were higher than those in XH [ $(13.8 \pm 16.7) \mu\text{mol}/(\text{m}^2 \cdot \text{d})$  for DIP and  $(200.5 \pm 158.2) \mu\text{mol}/(\text{m}^2 \cdot \text{d})$  for DSi], regardless of the spatial variations (Figs 5g, k, h and l). Such results indicate that the abundant organic matter in sediments contributes to the accumulation of inorganic nutrients via respiration and remineralization. The subse-

quent upward release of nutrients at the SWI plays a crucial role in maintaining the carbon and nitrogen biogeochemical processes such as photosynthesis and nitrification in the overlying water (Dan et al., 2021).

Boynton et al. (2018) have compiled the nutrient flux data at the SWI from different coastal ecosystems (such as bay, estuary, and lagoon) globally. We also supplemented the studies which published since 2018 with relation to SWI flux particularly in tropic regions (Table 1). The  $\text{NO}_x^-$ -N,  $\text{NH}_4^+$ -N, DIP, and DSi fluxes showed significant spatiotemporal variations among ecosystems and latitudes by several orders of magnitude (Table 1 and Boynton et al., 2018). In comparison, our nutrient fluxes at the SWI from tropical bays were within the range of the observations in mid to high latitude regions, but were 1–3 orders of magnitude lower than fluxes in some eutrophic regions (Table 1 and Boynton et al., 2018).

#### 4.2 Environmental regulators of nutrient fluxes at the sediment-water interface

Among the detected environmental factors, our correlation analysis indicated that water temperature, DO concentration, TOC and TN contents, C/N molar ratio, chlorophyll concentration, and sediment porosity were key regulators for the fluxes of inorganic nutrients at the SWI in tropical bays (Fig. 6). Temperature is one of the fundamental environmental factors regulating microbial activities and thus the carbon-nitrogen biogeochemical cycles. The positive correlation between the  $\text{NO}_x^-$ -N flux

**Table 1.** Comparison of nutrient fluxes at the sediment-water interface from different coastal regions globally

Study site	Type	Climate zone	Nutrient fluxes/ $(\mu\text{mol} \cdot \text{m}^{-2} \cdot \text{d}^{-1})$				Reference
			$\text{NH}_4^+$	$\text{NO}_x^-$	DIP	DSi	
Biscay Bay	bay	temperate	–453	528	200	–	Hulot et al., 2023
Bohai Bay	bay	temperate	–17.6	241.2	0.065	132.5	Mu et al., 2017
Gulf of Finland	gulf	temperate	590	40	2 580	–	Niemistö et al., 2018
Marano and Grado Lagoon	lagoon	temperate	1 080	305	–27.68	–9 630	Petranich et al., 2018
Long Island	estuary	temperate	$964.8 \pm 202.8$	$29.8 \pm 38.6$	$175.0 \pm 36.5$	–	Mazur et al., 2021
Brittany Mudflat	estuary	temperate	$2 424 \pm 2 808$	–	$408 \pm 480$	–	Louis et al., 2021
Daya Bay	bay	subtropic	$330 \pm 249$	–	$-1.3 \pm 16$	$549 \pm 301$	Zhang et al., 2019
Laguna de Términos	lagoon	tropic	$364.8 \pm 261.6$	$117.6 \pm 84.0$	$67.2 \pm 31.2$	$2 188.8 \pm 464.4$	Grenz et al., 2019
Mandovi River Estuary	estuary	tropic	18–2 370	220–660	–26–6	1–3 050	Pratihary et al., 2021
Amazon	estuary	tropic	683	–	26	–	Matos et al., 2020
Wisó River Estuary	estuary	tropic	–	17 545	4 110	–	Maslukah et al., 2019
Dongzhai Harbor (winter)	bay	tropic	51.6–807.7 $(207.3 \pm 248.2)$	–95.7–8.1 $(-50.2 \pm 26.5)$	–	–	This study
Dongzhai Harbor (summer)	bay	tropic	18.9–687.7 $(317.9 \pm 311.0)$	–39.2–176.4 $(12.4 \pm 64.0)$	–	–	This study
Xiaohai Lagoon	lagoon	tropic	204.0–3 520.8 $(1 067.9 \pm 945.6)$	–21.7–23.4 $(-1.2 \pm 13.1)$	–3.7–73.3 $(13.8 \pm 16.7)$	–26.9–297.8 $(200.5 \pm 158.2)$	This study
Qinglan Harbor	lagoon	tropic	12.4–8 790.6 $(1 378.6 \pm 2 444.4)$	–0.5–186.0 $(20.6 \pm 52.3)$	–0.6–103 $(28.8 \pm 32.8)$	35.9–522.2 $(294.2 \pm 283.2)$	This study

Note: – represents no data.

and temperature (Fig. 6) may suggest that rising temperature stimulates the sediment organic matter respiration and nitrification, leading to the accumulation of nitrate in porewater and promoting its diffusion into the overlying water. Temperature manipulation experiments also found that an increase in temperature within a certain range can enhance the sediment  $\text{NO}_x^-$ -N efflux (Zhu et al., 2023). The DO concentration in water determines the oxygen penetration depth in sediments, regulating aerobic respiration and the release of inorganic nutrients at the SWI (Boynton et al., 2018). However, we only observed a negative correlation between  $\text{NO}_x^-$ -N flux and DO (Fig. 6) may be due to the small variations in oxygen concentration during our cruises (Fig. 2d).

The fluxes of  $\text{NH}_4^+$ -N, DIP and DSi at the SWI showed significant positive correlations with the concentrations of TOC, TN and Chl *a* in sediments (Fig. 6). The  $\text{NH}_4^+$ -N flux negatively correlated with the C/N ratio (Fig. 6). These results indicated that both the quality and quantity of organic matter govern the nutrients exchange at the SWI. Labile organic matter drives various biogeochemical processes and then the release of inorganic nutrients, especially the  $\text{NH}_4^+$ -N, DIP and DSi, in sediments by supplying energy and substrates (Percuoco et al., 2015).

The sediment  $\text{NO}_x^-$ -N flux was positively correlated to C/N ratio (Fig. 6), suggesting that fresh organic matter with low C/N ratio prefers to remove  $\text{NO}_x^-$ -N via promoting the coupled nitrification-denitrification processes in sediments (Tan et al., 2022).

Salinity is a proxy for the nutrients concentration in overlying water and thus can act as one of the controlling factors for nutrients exchange at the SWI (Lin et al., 2013). Meanwhile, salinity regulates the SWI flux by altering the microbial community in sediments (Gardner et al., 1991). However, we observed no correlations between flux and salinity (Fig. 6) may be due to the narrow salinity variation in the study regions (25.7–32.3 in DZG and 25.5–33.1 in QLG, excepting for XH with a range of 10.7–33.0; Fig. 2c). The porosity, which is determined by the sediment particle size, directly determines the permeability regulating the molecular diffusion process of nutrients in sediments (Wan et al., 2023). The highly permeable sediment is conducive to nutrient exchange at the SWI (Fig. 6). Currently, most of the related studies focus on nutrient exchange at the SWI of muddy sediments with low permeability (Boynton et al., 2018). However, the permeable sediment accounts for more than 50% of sediment area in marginal seas (Hall, 2002). The source/sink

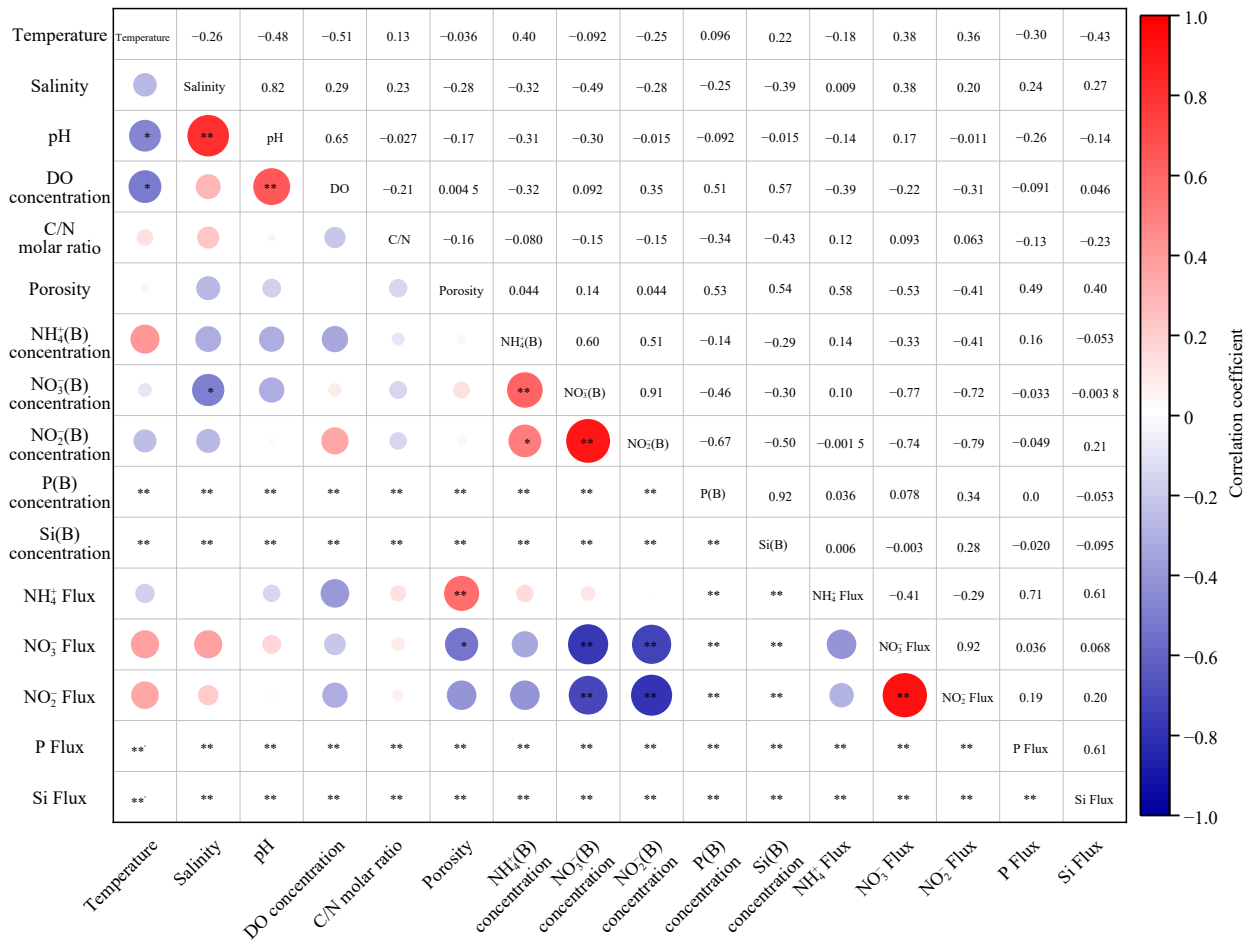


Fig. 6. Pearson's correlation analysis between nutrient flux at the sediment-water interface and the detected environmental parameters. \*,  $p < 0.05$ ; \*\*,  $p < 0.01$ .

structure of nutrients exchange at the SWI and their ecological and biogeochemical impacts in these ecosystems need further quantitative assessment. In addition, finer sediments organic matter with high quality, thereby influencing the production, absorption, desorption of nutrients, and their fluxes at the SWI (Huang et al., 2022; van Rijn, 1984).

This study only explored the influence of environmental factors on the physically diffusion-derived SWI fluxes. In actual environments, bioturbation, irrigation and tide-induced sediment resuspension are also crucial factors to promote/inhibit the nutrient exchange at the sediment-water interface. Mu et al. (2017) have found a significant increase in nutrient fluxes at the SWI after the addition of biology inhibitor. McTigue et al. (2016) also indicated that bioturbation enhances the sediment denitrification to remove nitrate in Arctic shelves. We need to evaluate the effects of these macrobiotic activity on SWI nutrient exchange in the future.

#### 4.3 The importance of sediment-water interface fluxes to the nutrient sources in tropic bays

The average DIN/DIP molar ratios in bottom water in XH and QLG were  $8.5 \pm 12.4$  and  $8.0 \pm 7.0$  (Table 2), respectively, indicating a nitrogen-limited ecosystem when considering a 16:1 of N/P ratio for phytoplankton assimilation (Redfield, 1958). However, the average DIN/DIP ratios in porewater ranged from 16.8 to 29.1 (Table 2), which were 3 times higher than the N/P ratios in the bottom water. Notably, the sediments act as a source for the DIN, DIP and DSi in these three tropical bays. Here the DIN flux was calculated by the sum of  $\text{NH}_4^+$ -N and  $\text{NO}_x^-$ -N fluxes. The sedimentary nutrients input with high N/P ratio will alter the structure of nutrient composition in

overlying water (Díez et al., 2013), mitigating the nitrogen limitation and influencing the phytoplankton communities and subsequent carbon sink in coastal ecosystems (Lee et al., 2010; Oelsner and Stets, 2019).

To assess the relative importance of the SWI fluxes to the total nutrient input, we collected historical data on the other external nutrient sources, including river input, submarine groundwater discharge (SGD), and atmospheric deposition in XH and QLG (the DZG lacks the external inputs data). In XH, the SWI fluxes of DIN, DIP, and DSi were 2–4 orders of magnitude lower than nutrient fluxes from river and SGD, but were 4, 8, and 20 times higher than the atmospheric deposition for DIN, DIP, and DSi fluxes, respectively (Table 3). In contrast, the DIN, DIP, and DSi fluxes at the SWI were nearly one order of magnitude lower than riverine and SGD fluxes, and comparable to the atmospheric deposition (Table 3). Such comparison results suggested that river input and SGD were two primary sources of inorganic nutrients, with a minor contribution from SWI in these two bays.

#### 4.4 The interpretation of data on nutrient fluxes at the global marine sediment-water interface

According to our tropical nutrient fluxes and the compilation in Boynton et al. (2018), the sediments basically act as a source for  $\text{NH}_4^+$ -N, DIP, and DSi with substantial temporal and spatial variations. While for  $\text{NO}_x^-$ -N, the sediments can be a source or sink in coastal ecosystems with shallow water depth (<20 m), but in deep water environments (>20 m), the sediments are generally a sink for nitrate (Boynton et al., 2018). The exchange direction and flux of nutrients at the SWI are largely determined by the concentration difference between porewater and overlying

**Table 2.** The stoichiometry of DIN and DIP in bottom water and porewater at Dongzhai Harbor, Xiaohai Lagoon and Qinglan Harbor in different seasons

Study site	Season	Bottom water		Porewater	
		DIN/DIP molar ratio	Average	DIN/DIP molar ratio	Average
Dongzhai Harbor	Winter	NA	NA	8.5–42.8	$16.8 \pm 10.6$
Dongzhai Harbor	Summer	NA	NA	6.3–35.8	$17.3 \pm 10.4$
Xiaohai Lagoon	Summer	0.1–45.8	$8.5 \pm 12.4$	6.6–56.2	$29.1 \pm 13.9$
Qinglan Harbor	Summer	1.3–23.6	$8.0 \pm 7.0$	5.1–72.7	$26.2 \pm 21.9$

Note: NA represents not applicable.

**Table 3.** Comparison of nutrient fluxes from different sources including the SWI flux, SGD flux, river input and atmospheric deposition in Xiaohai Lagoon (XH) and Qinglan Harbor (QLG), unit in  $10^4$  mol/d

		DIN	DIP	DSi	Reference
XH	SWI flux	$4.3 \pm 4.2$	$0.08 \pm 0.09$	$0.6 \pm 0.5$	This study
	SGD flux	157.0	8.5	2 561.6	Wang and Du, 2016
	River input	183.6	2.4	275.3	Wang and Du, 2016
	Atmospheric deposition	1.2	0.01	0.03	Wang and Du, 2016
QLG	SWI flux	$2.8 \pm 4.9$	$0.07 \pm 0.07$	$0.4 \pm 0.3$	This study
	SGD flux	$15.5 \pm 25.1$	$0.17 \pm 0.38$	$12.1 \pm 18.4$	Su et al., 2011
	River input	$13.4 \pm 6.6$	$0.12 \pm 0.07$	$24.7 \pm 3.6$	Liu et al., 2011
	Atmospheric deposition	$4.3 \pm 7.6$	$0.15 \pm 0.22$	$3.6 \pm 3.0$	Liu et al., 2011

ing water. We thus proposed that primary production in overlying water and external nutrient inputs interpret the

conversion between source and sink for nutrients (particularly for nitrate) exchange at the SWI in marine ecosys-

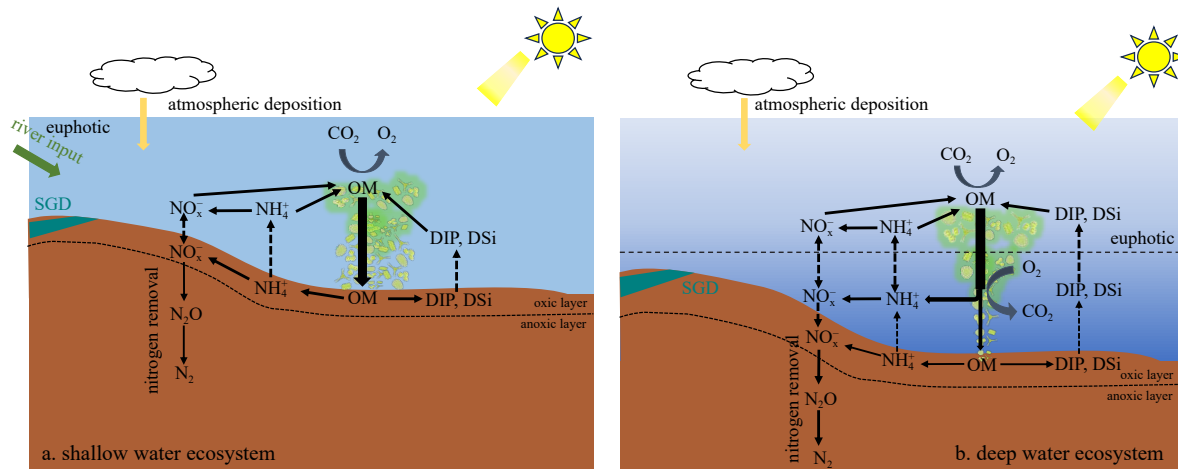


**Fig. 7.** The conceptual diagram of the effects of external inputs and primary production on nutrient exchange at the SWI in shallow water (a) and deep water ecosystems (b).

tems with different water depths (Fig. 7).

In coastal shallow water ecosystems, the abundant light and eutrophic environments are conducive to the primary production to consume nutrients in the entire water column. Most of the terrigenous and local produced organic matter is buried and degraded in coastal sediments and contributes to the accumulation of inorganic nutrients in porewater. The  $\text{NO}_x^-$ -N exchange at the SWI in this scenario depends on the external nitrate source including riverine input, SGD and atmospheric deposition (Fig. 7a). The sediment exhibits a nitrate sink especially in eutrophic environments (e.g., upstream estuaries) with adequate external nutrient supply, while the sediment releases nitrate to the water in environments with no or low external nutrient supply (Fig. 7a). In deep-water ecosystems, large part of photosynthesis-produced organic matter in euphotic zone will degrade into inorganic nutrients in the aphotic zone and then accumulated in bottom water. Only a small proportion of organic matter settles to the surface sediment to restrict nitrate accumulation in porewater. The sediments thus adsorb and remove  $\text{NO}_x^-$ -N from the overlying water (Fig. 7b). For the  $\text{NH}_4^+$ -N, DIP, and DSi, the  $\text{NH}_4^+$ -N is easily nitrified to nitrate and thus difficult to accumulate in the bottom water (Hutchins and Capone, 2022). Both DIP and DSi are more likely to be preserved in sediments due to their own biochemical characteristics (Ingri et al., 1991; Spiteri et al., 2008). As a result, sediment usually acts as a source for these three inorganic nutrients regardless of the regions (Fig. 7).

## 5 Conclusions

We quantitatively assess the exchange of  $\text{NO}_x^-$ -N,  $\text{NH}_4^+$ -N, DIP, and DSi at the SWI in three tropical bays. Sediments act as a source of  $\text{NH}_4^+$ -N, DIP, and DSi, but for  $\text{NO}_x^-$ -N, sediments can be both a source and sink, al-

though with substantial spatial and temporal variations in their fluxes. Labile organic matter is a critical regulator for the fluxes of inorganic nutrient at the SWI. The sedimentary nutrients input with high N/P ratio will alter the structure of nutrient composition to mitigate the nitrogen limitation in coastal waters. However, the internal sediment release in these tropical bays plays a relative weak role in contributing to the nutrient addition in comparison with the other external nutrient sources such as riverine input, SGD, and atmospheric deposition. Integrating our findings into global compilation in Boynton et al. (2018), we propose that water column primary production and external inputs to interpret the variation in exchange and fluxes of nutrients at the SWI in different ecosystems. Such an understanding of these chain biogeochemical processes involving external nutrient input, primary production, particulate organic matter settling, and the accumulation and release of inorganic nutrients in sediments will be helpful for the scientific-based pollution prevent and control in coastal waters.

## References

- Behrenfeld M J, O'Malley R T, Siegel D A, et al. 2006. Climate-driven trends in contemporary ocean productivity. *Nature*, 444(7120): 752–755, doi: [10.1038/nature05317](https://doi.org/10.1038/nature05317)
- Ben Mna H, Alsubih M, Oueslati W, et al. 2022. Diagenetic processes and nutrients diffusive fluxes at the sediment-water interface in the Bizerte Lagoon (North Tunisia). *Journal of African Earth Sciences*, 196: 104671, doi: [10.1016/j.jafrearsci.2022.104671](https://doi.org/10.1016/j.jafrearsci.2022.104671)
- Boudreau B P. 1997. *Diagenetic Models and Their Implementation: Modelling Transport and Reactions in Aquatic Sediments*. Berlin, Heidelberg: Springer, 1–398
- Boynton W R, Ceballos M A C, Bailey E M, et al. 2018. Oxygen and nutrient exchanges at the sediment-water inter-

- face: a global synthesis and critique of estuarine and coastal data. *Estuaries and Coasts*, 41(2): 301–333, doi: [10.1007/s12237-017-0275-5](https://doi.org/10.1007/s12237-017-0275-5)
- Burdige D J. 2011. Estuarine and coastal sediments—Coupled biogeochemical cycling. In: Mcluskay D, Wolanski E, eds. *Treatise on Estuarine and Coastal Science*. Amsterdam: Academic Press, 279–316
- Chen Xiaohua, Chen Zongzhu, Lei Jinrui, et al. 2022. Distribution characteristics of active organic carbon components in sediments of typical community types of mangrove wetland in Qinglan Port. *Acta Ecologica Sinica* (in Chinese), 42(11): 4572–4581
- Chen Shigan, Teng Junhua. 1996. Preliminary study of distribution of fringing reef at Qinglan Bay and eastern coast, Hainan Island. *Journal of Oceanography in Taiwan Strait* (in Chinese), 15(1): 75–80
- Dadi T, Friese K, Wendt-Potthoff K, et al. 2023. Oxygen dependent temperature regulation of benthic fluxes in reservoirs. *Global Biogeochemical Cycles*, 37(4): e2022GB007647, doi: [10.1029/2022GB007647](https://doi.org/10.1029/2022GB007647)
- Dan S F, Li Shengyong, Yang Bin, et al. 2021. Influence of sedimentary organic matter sources on the distribution characteristics and preservation status of organic carbon, nitrogen, phosphorus, and biogenic silica in the Daya Bay, northern South China Sea. *Science of the Total Environment*, 783: 146899, doi: [10.1016/j.scitotenv.2021.146899](https://doi.org/10.1016/j.scitotenv.2021.146899)
- Denis L, Grenz C. 2003. Spatial variability in oxygen and nutrient fluxes at the sediment-water interface on the continental shelf in the Gulf of Lions (NW Mediterranean). *Oceanologica Acta*, 26(4): 373–389, doi: [10.1016/S0399-1784\(03\)00017-3](https://doi.org/10.1016/S0399-1784(03)00017-3)
- Devlin M, Brodie J. 2023. Nutrients and eutrophication. In: Reichelt-Brushett A, ed. *Marine Pollution—Monitoring, Management and Mitigation*. Cham: Springer, 75–100
- Devol A H. 2015. Denitrification, anammox, and N<sub>2</sub> production in marine sediments. *Annual Review of Marine Science*, 7: 403–423, doi: [10.1146/annurev-marine-010213-135040](https://doi.org/10.1146/annurev-marine-010213-135040)
- Díez B, Nieuwerburgh L V, Snoeijs P. 2013. Water nutrient stoichiometry modifies the nutritional quality of phytoplankton and somatic growth of crustacean mesozooplankton. *Marine Ecology Progress Series*, 489: 93–105, doi: [10.3354/meps10438](https://doi.org/10.3354/meps10438)
- Fennel K, Testa J M. 2019. Biogeochemical controls on coastal hypoxia. *Annual Review of Marine Science*, 11(1): 105–130, doi: [10.1146/annurev-marine-010318-095138](https://doi.org/10.1146/annurev-marine-010318-095138)
- Gardner W S, Seitzinger S P, Malczyk J M. 1991. The effects of sea salts on the forms of nitrogen released from estuarine and freshwater sediments: Does ion pairing affect ammonium flux?. *Estuaries*, 14(2): 157–166, doi: [10.2307/1351689](https://doi.org/10.2307/1351689)
- Gong Wenping, Shen Jian, Jia Jianjun. 2008. The impact of human activities on the flushing properties of a semi-enclosed lagoon: Xiaohai, Hainan, China. *Marine Environmental Research*, 65(1): 62–76, doi: [10.1016/j.marenvres.2007.08.001](https://doi.org/10.1016/j.marenvres.2007.08.001)
- Grenz C, Moreno M O, Soetaert K, et al. 2019. Spatio-temporal variability in benthic exchanges at the sediment-water interface of a shallow tropical coastal lagoon (south coast of Gulf of Mexico). *Estuarine, Coastal and Shelf Science*, 218: 368–380
- Hall S J. 2002. The continental shelf benthic ecosystem: current status, agents for change and future prospects. *Environmental Conservation*, 29(3): 350–374, doi: [10.1017/S0376892902000243](https://doi.org/10.1017/S0376892902000243)
- Huang Lei, Gao Qifeng, Fang Hongwei, et al. 2022. Effects of bedform migration on nutrient fluxes at the sediment–water interface: a theoretical analysis. *Environmental Fluid Mechanics*, 22(2): 447–466
- Hulot V, Metzger E, Thibault de Chanvalon A, et al. 2023. Impact of an exceptional winter flood on benthic oxygen and nutrient fluxes in a temperate macrotidal estuary: Potential consequences on summer deoxygenation. *Frontiers in Marine Science*, 10: 1083377, doi: [10.3389/fmars.2023.1083377](https://doi.org/10.3389/fmars.2023.1083377)
- Hutchins D A, Capone D G. 2022. The marine nitrogen cycle: new developments and global change. *Nature Reviews Microbiology*, 20(7): 401–414, doi: [10.1038/s41579-022-00687-z](https://doi.org/10.1038/s41579-022-00687-z)
- Ingri J, Löfvendahl R, Boström K. 1991. Chemistry of suspended particles in the southern Baltic Sea. *Marine Chemistry*, 32(1): 73–87, doi: [10.1016/0304-4203\(91\)90026-S](https://doi.org/10.1016/0304-4203(91)90026-S)
- Lee Y W, Kim G, Lim W A, et al. 2010. A relationship between submarine groundwater borne nutrients traced by Ra isotopes and the intensity of dinoflagellate red-tides occurring in the southern sea of Korea. *Limnology and Oceanography*, 55(1): 1–10, doi: [10.4319/lo.2010.55.1.0001](https://doi.org/10.4319/lo.2010.55.1.0001)
- Lehrter J C, Beddick D L, Devereux R, et al. 2012. Sediment-water fluxes of dissolved inorganic carbon, O<sub>2</sub>, nutrients, and N<sub>2</sub> from the hypoxic region of the Louisiana continental shelf. *Biogeochemistry*, 109(1): 233–252
- Li Shiping, Li Xian, Zhang Guanglei, et al. 2017. Study on water quality and change trends in the mariculture zone of Dongzhaigang. *Journal of Hainan Normal University: Natural Science* (in Chinese), 30(4): 430–435
- Lin Genmei, Lin Xianbiao. 2022. Bait input altered microbial community structure and increased greenhouse gases production in coastal wetland sediment. *Water Research*, 218: 118520, doi: [10.1016/j.watres.2022.118520](https://doi.org/10.1016/j.watres.2022.118520)
- Lin Peng, Guo Laodong, Chen Min, et al. 2013. Distribution, partitioning and mixing behavior of phosphorus species in the Jiulong River Estuary. *Marine Chemistry*, 157: 93–105
- Liu Sumei, Hong Gi-Hoon, Zhang Jing, et al. 2009. Nutrient budgets for large Chinese estuaries. *Biogeosciences*, 6(10): 2245–2263, doi: [10.5194/bg-6-2245-2009](https://doi.org/10.5194/bg-6-2245-2009)
- Liu Sumei, Li Ruihuan, Zhang Guiling, et al. 2011. The impact of anthropogenic activities on nutrient dynamics in the tropical Wenchanghe and Wenjiaohe Estuary and Lagoon system in East Hainan, China. *Marine Chemistry*, 125(1–4): 49–68, doi: [10.1016/j.marchem.2011.02.003](https://doi.org/10.1016/j.marchem.2011.02.003)
- Louis J, Jeanneau L, Andrieux-Loyer F, et al. 2021. Are benthic nutrient fluxes from intertidal mudflats driven by sur-

- face sediment characteristics?. *Comptes Rendus. Géoscience*, 353(1): 173–191
- Luo Lizhen, Zhu Zhixiong, Chen Shiquan, et al. 2022. Spatial distribution and contamination evaluation of surface sediment in Xiaohai, Wanning. *Transactions of Oceanology and Limnology (in Chinese)*, 44(2): 103–111
- Mackenzie F T, Ver L M, Lerman A. 2002. Century-scale nitrogen and phosphorus controls of the carbon cycle. *Chemical Geology*, 190(1–4): 13–32, doi: [10.1016/S0009-2541\(02\)00108-0](https://doi.org/10.1016/S0009-2541(02)00108-0)
- Maslukah L, Wulandari S Y, Prasetyawan I B, et al. 2019. Distributions and fluxes of nitrogen and phosphorus nutrients in porewater sediments in the estuary of Jepara Indonesia. *Journal of Ecological Engineering*, 20(2): 58–64, doi: [10.12911/22998993/95093](https://doi.org/10.12911/22998993/95093)
- Matos C R L, Berrêdo J F, Machado W, et al. 2020. Carbon and nutrient accumulation in tropical mangrove creeks, Amazon region. *Marine Geology*, 429: 106317, doi: [10.1016/j.margeo.2020.106317](https://doi.org/10.1016/j.margeo.2020.106317)
- Mazur C I, Al-Haj A N, Ray N E, et al. 2021. Low denitrification rates and variable benthic nutrient fluxes characterize Long Island Sound sediments. *Biogeochemistry*, 154(1): 37–62, doi: [10.1007/s10533-021-00795-7](https://doi.org/10.1007/s10533-021-00795-7)
- McTigue N D, Gardner W S, Dunton K H, et al. 2016. Biotic and abiotic controls on co-occurring nitrogen cycling processes in shallow Arctic shelf sediments. *Nature Communications*, 7(1): 13145, doi: [10.1038/ncomms13145](https://doi.org/10.1038/ncomms13145)
- Mu Di, Yuan Dekui, Feng Huan, et al. 2017. Nutrient fluxes across sediment-water interface in Bohai Bay Coastal Zone, China. *Marine Pollution Bulletin*, 114(2): 705–714, doi: [10.1016/j.marpolbul.2016.10.056](https://doi.org/10.1016/j.marpolbul.2016.10.056)
- Niemistö J, Kononets M, Ekeröth N, et al. 2018. Benthic fluxes of oxygen and inorganic nutrients in the archipelago of Gulf of Finland, Baltic Sea—Effects of sediment resuspension measured *in situ*. *Journal of Sea Research*, 135: 95–106, doi: [10.1016/j.seares.2018.02.006](https://doi.org/10.1016/j.seares.2018.02.006)
- Nriagu J O. 1979. *Geochemical processes, water and sediment environments: A. Lerman*. Wiley, 1979, 481 pp. \$29.95. *Geochimica et Cosmochimica Acta*, 43(11): 1869–1870
- Oelsner G P, Stets E G. 2019. Recent trends in nutrient and sediment loading to coastal areas of the conterminous U. S.: Insights and global context. *Science of the Total Environment*, 654: 1225–1240, doi: [10.1016/j.scitotenv.2018.10.437](https://doi.org/10.1016/j.scitotenv.2018.10.437)
- Percuoco V P, Kalnejais L H, Officer L V. 2015. Nutrient release from the sediments of the Great Bay Estuary, N. H. USA. *Estuarine, Coastal and Shelf Science*, 161: 76–87
- Petranich E, Covelli S, Acquavita A, et al. 2018. Benthic nutrient cycling at the sediment-water interface in a lagoon fish farming system (northern Adriatic Sea, Italy). *Science of the Total Environment*, 644: 137–149, doi: [10.1016/j.scitotenv.2018.06.310](https://doi.org/10.1016/j.scitotenv.2018.06.310)
- Pinckney J, Papa R, Zingmark R. 1994. Comparison of high-performance liquid chromatographic, spectrophotometric, and fluorometric methods for determining chlorophyll *a* concentrations in estuarine sediments. *Journal of Microbiological Methods*, 19(1): 59–66, doi: [10.1016/0167-7012\(94\)90026-4](https://doi.org/10.1016/0167-7012(94)90026-4)
- Pinsky M L, Eikeset A M, McCauley D J, et al. 2019. Greater vulnerability to warming of marine versus terrestrial ectotherms. *Nature*, 569(7754): 108–111, doi: [10.1038/s41586-019-1132-4](https://doi.org/10.1038/s41586-019-1132-4)
- Pratihary A, Naik R, Karapurkar S, et al. 2021. Benthic exchange along a tropical estuarine salinity gradient during dry season: Biogeochemical and ecological implications. *Journal of Sea Research*, 177: 102124, doi: [10.1016/j.seares.2021.102124](https://doi.org/10.1016/j.seares.2021.102124)
- Qiu Huimin, Geng Jinju, Ren Hongqiang, et al. 2016. Phosphate flux at the sediment-water interface in northern Lake Taihu. *Science of the Total Environment*, 543: 67–74, doi: [10.1016/j.scitotenv.2015.10.136](https://doi.org/10.1016/j.scitotenv.2015.10.136)
- Redfield A C. 1958. The biological control of chemical factors in the environment. *American Scientist*, 46(3): 205–221
- Seitzinger S, Harrison J A, Böhlke J K, et al. 2006. Denitrification across landscapes and waterscapes: a synthesis. *Ecological Applications*, 16(6): 2064–2090, doi: [10.1890/1051-0761\(2006\)016\[2064:DALAWA\]2.0.CO;2](https://doi.org/10.1890/1051-0761(2006)016[2064:DALAWA]2.0.CO;2)
- Spiteri C, van Cappellen P, Regnier P. 2008. Surface complexation effects on phosphate adsorption to ferric iron oxyhydroxides along pH and salinity gradients in estuaries and coastal aquifers. *Geochimica et Cosmochimica Acta*, 72(14): 3431–3445, doi: [10.1016/j.gca.2008.05.003](https://doi.org/10.1016/j.gca.2008.05.003)
- Su Ni, Du Jinzhou, Moore W S, et al. 2011. An examination of groundwater discharge and the associated nutrient fluxes into the estuaries of eastern Hainan Island, China using <sup>226</sup>Ra. *Science of the Total Environment*, 409(19): 3909–3918, doi: [10.1016/j.scitotenv.2011.06.017](https://doi.org/10.1016/j.scitotenv.2011.06.017)
- Tan Ehui, Hsu Ting-Chang, Zou Wenbin, et al. 2022. Quantitatively deciphering the roles of sediment nitrogen removal in environmental and climatic feedbacks in two subtropical estuaries. *Water Research*, 224: 119121, doi: [10.1016/j.watres.2022.119121](https://doi.org/10.1016/j.watres.2022.119121)
- Tan Ehui, Zou Wenbin, Jiang Xinlei, et al. 2019. Organic matter decomposition sustains sedimentary nitrogen loss in the Pearl River Estuary, China. *Science of the Total Environment*, 648: 508–517, doi: [10.1016/j.scitotenv.2018.08.109](https://doi.org/10.1016/j.scitotenv.2018.08.109)
- Thamdrup B, Dalsgaard T. 2008. Nitrogen cycling in sediments. In: Kirchman D L, ed. *Microbial Ecology of the Oceans*. 2nd ed. Hoboken: John Wiley & Sons, 527–568
- Ullman W J, Aller R C. 1982. Diffusion coefficients in nearshore marine sediments. *Limnology and Oceanography*, 27(3): 552–556, doi: [10.4319/lo.1982.27.3.0552](https://doi.org/10.4319/lo.1982.27.3.0552)
- Van Rijn L C. 1984. Sediment transport, Part III: Bed forms and alluvial roughness. *Journal of Hydraulic Engineering*, 110(12): 1733–1754, doi: [10.1061/\(ASCE\)0733-9429\(1984\)110:12\(1733\)](https://doi.org/10.1061/(ASCE)0733-9429(1984)110:12(1733))
- Wan Ru, Ge Lianghao, Chen Bin, et al. 2023. Permeability decides the effect of antibiotics on sedimentary nitrogen removal in Jiulong River Estuary. *Water Research*, 243: 120400, doi: [10.1016/j.watres.2023.120400](https://doi.org/10.1016/j.watres.2023.120400)
- Wang Xilong, Du Jinzhou. 2016. Submarine groundwater dis-

- charge into typical tropical lagoons: A case study in eastern Hainan Island, China. *Geochemistry, Geophysics, Geosystems*, 17(11): 4366–4382
- Wang Huan, Li Qi, Xu Jun. 2023. Climate warming does not override eutrophication, but facilitates nutrient release from sediment and motivates eutrophic process. *Microorganisms*, 11(4): 910, doi: [10.3390/microorganisms11040910](https://doi.org/10.3390/microorganisms11040910)
- Zhang Ling, Wang Lu, Yin Kedong, et al. 2014. Spatial and seasonal variations of nutrients in sediment profiles and their sediment-water fluxes in the Pearl River Estuary, Southern China. *Journal of Earth Science*, 25(1): 197–206, doi: [10.1007/s12583-014-0413-y](https://doi.org/10.1007/s12583-014-0413-y)
- Zhang Ling, Xiong Lanlan, Zhang Jingping, et al. 2019. The benthic fluxes of nutrients and the potential influences of sediment on the eutrophication in Daya Bay, South China. *Marine Pollution Bulletin*, 149: 110540, doi: [10.1016/j.marpolbul.2019.110540](https://doi.org/10.1016/j.marpolbul.2019.110540)
- Zhang Xiaoli, Yao Cheng, Zhang Bosong, et al. 2023. Dynamics of benthic nitrate reduction pathways and associated microbial communities responding to the development of seasonal deoxygenation in a coastal mariculture zone. *Environmental Science & Technology*, 57(40): 15014–15025
- Zhao Haichao, Zhang Li, Wang Shengrui, et al. 2018. Features and influencing factors of nitrogen and phosphorus diffusive fluxes at the sediment-water interface of Erhai Lake. *Environmental Science and Pollution Research*, 25(2): 1933–1942, doi: [10.1007/s11356-017-0556-3](https://doi.org/10.1007/s11356-017-0556-3)
- Zhen Jianing, Liao Jingjuan, Shen Guozhuang. 2019. Remote sensing monitoring and analysis on the dynamics of mangrove forests in Qinglan Harbor of Hainan Province since 1987. *Wetland Science (in Chinese)*, 17(1): 44–51
- Zhou Nan, Zhang Guoling, Liu Sumei. 2022. Nutrient exchanges at the sediment-water interface and the responses to environmental changes in the Yellow Sea and East China Sea. *Marine Pollution Bulletin*, 176: 113420, doi: [10.1016/j.marpolbul.2022.113420](https://doi.org/10.1016/j.marpolbul.2022.113420)
- Zhu Dantong, Cheng Xiangju, Sample D J, et al. 2023. Effect of water temperature on internal nitrogen release from sediments in the Pearl River Delta region, China. *Hydrology Research*, 54(9): 1055–1071, doi: [10.2166/nh.2023.056](https://doi.org/10.2166/nh.2023.056)